Calcium-sensing Receptor is not Expressed in the Absorptive Enterocytes of Weaned Piglets[1]

Xiaoya Zhao,[*] Qianru Hui,[*] Paula Azevedo,[*] Charles Martin Nyachoti, [*] Karmin O, [*†] Chengbo Yang [*2]

*Department of Animal Science, University of Manitoba, Winnipeg, Manitoba, Canada, R3T 2N2;

†CCARM, St. Boniface Hospital Research Centre, Winnipeg, Manitoba, Canada, R2H 2A6

[1]This work was supported by the Natural Sciences and Engineering Council of Canada (NSERC) Discovery Grants (C. Yang: RGPIN-2017-04967), Canada foundation for innovation (CFI), the University of Manitoba Start-Up Grant, the Graduate Enhancement of Tri-Council Stipends (GETS) program at the University of Manitoba. The authors are grateful to Christine Zhang at the University of Manitoba for the fluorescence-activated cell sorting.

[2]*Corresponding author: Chengbo Yang: chengbo.yang@umanitoba.ca*

LAY SUMMARY

The calcium-sensing receptor (CaSR) has been identified as a nutrient sensor along the gastrointestinal tract and plays a pivotal role in food digestion, nutrient absorption, and energy metabolism. Hence, elucidating the expression pattern of pig CaSR (pCaSR) in the intestinal segments, especially in the absorptive enterocytes, could reveal the significance of pCaSR in nutrient sensing in the gastrointestinal tract. In the present work, after isolating enterocytes from the ileum of weaned piglets, we investigated the expression of pCaSR in porcine enterocytes through a combination of biological tools at both gene and protein expression levels. Data observed in the current study revealed that porcine enterocytes could be obtained by using cell sorting with a digestive enzyme (sucrase-isomaltase) as the enterocyte-specific marker. Plus, the pCaSR is not expressed in either isolated porcine ileal enterocytes or the porcine jejunal enterocyte cell line (IPEC-J2).

TEASER TEXT

We isolated enterocytes from the ileum of weaned piglets by using sucrase-isomaltase as an enterocyte-specific marker and investigated the expression of CaSR in porcine primary enterocytes and the enterocyte-like cell line IPEC-J2. Our findings suggested no expression of pCaSR in both porcine ileal enterocytes and IPEC-J2 cells.

ABSTRACT:

The calcium-sensing receptor (CaSR) is a kokumi receptor that plays an essential role in nutrient sensing and animal physiology, growth, and development. Pig CaSR (pCaSR) was identified and characterized in the intestine. However, further research is still needed to confirm the expression of CaSR in the epithelial cells isolated from weaned piglets. In this study, primary enterocytes were isolated and characterized from the ileum of weaned piglets by the Weiser distended intestinal sac technique and fluorescence-activated cell sorting (FACS) based on sucrase-isomaltase as an enterocyte-specific marker. The expression of CaSR was investigated in both primary enterocytes and the intestinal porcine enterocyte cell line (IPEC-J2) by droplet digital PCR (ddPCR), immunofluorescence staining, and western blotting. Results demonstrated that porcine enterocytes could be obtained using FACS with the sucrase-isomaltase as the enterocyte-specific marker and that pCaSR is not expressed in both porcine ileal enterocytes and IPEC-J2 cells, which specifically identified the expression of pCaSR in ileal enterocytes with sensitive and specific approaches.

KEYWORDS:

Calcium-sensing receptor; enterocytes; enteroendocrine cells; IPEC-J2; weaned piglets

ABBREVIATIONS

AM	apical membrane
BLM	basolateral membrane
cAMP	cyclic adenosine monophosphate
CaSR	calcium-sensing receptor
CCK	cholecystokinin
DAPI	4′,6-diamidino-2-phenylindole
ddPCR	droplet digital PCR
DTT	dithiothreitol
DMEM	dulbecco's modified eagle medium
EECs	enteroendocrine cells
EDTA	ethylenediaminetetraacetic acid
FACS	fluorescence-activated cell sorting
FBS	fetal bovine serum
GLP-1	glucagon-like peptide 1
GLP-2	glucagon-like peptide 2
GPCRs	G protein-coupled receptors
HEK 293	human embryonic kidney 293
IPEC-J2	intestinal porcine epithelial cell line-j2
PBS	phosphate-buffered saline

pCaSR	pig calcium-sensing receptor
PMSF	phenylmethylsulfonyl fluoride
PKA	protein kinase A
PKC	protein kinase C
PYY	peptide YY
SI	sucrase-isomaltase

INTRODUCTION

The calcium-sensing receptor (CaSR) is a kokumi receptor that plays important roles in nutrient sensing and in the physiology, growth, and development of animals. To further elucidate the molecular and physiological roles of pig CaSR (pCaSR) in intestinal nutrient sensing in pigs, it is important to investigate the molecular distribution and localization of pCaSR in specific tissues such as the small intestine and cell types. In our previous study, the pCaSR was identified and characterized in pigs, and its expression in several tissues such as the intestine was confirmed (Zhao et al., 2019). Specifically, within the intestine, the ileum has the highest expression level of pCaSR (Zhao et al., 2019).

The intestinal epithelium is lined with a single layer of epithetical cells including polarized absorptive enterocytes, goblet cells, enteroendocrine cells (EECs), and Paneth cells (Umar, 2010). Enterocytes constitute the majority (85%) of the cells lining the villus, while EECs represent 1% of the cells (Bullen et al., 2006; Busslinger et al., 2021). The expression of taste receptors like CaSR has been identified in the EECs (Ohsu et al., 2010). However, the taste receptor family (taste receptor type 1 member 1 (T1R1), T1R2, and T1R3) also was found in absorptive enterocytes except for EECs (Mace et al., 2007). Plus, CaSR has been found in commercial enterocyte cell lines such as Caco-2 and HT-29 (Mine and Zhang, 2015b; Zhang et al., 2015b). As stated previously, absorptive enterocytes constitute most of the intestinal epithelial cells, and positive immunolocalization of pCaSR was observed in the epithelium of the gastrointestinal tract, with the most abundant mRNA level in the ileum. Thus, we hypothesize that pCaSR is expressed in both absorptive enterocytes and EECs in the intestine of pigs, as shown in Figure 1. In this study, primary enterocytes were isolated and characterized from the ileum of weaned piglets, and the expression of CaSR was investigated in both primary enterocytes and the intestinal porcine enterocyte cell line (IPEC-J2).

MATERIAL AND METHODS

The experimental and animal care protocols (F17-018, AC11280) were reviewed and approved by the Animal Care Committee of the University of Manitoba, and piglets were cared for following the Canadian Council on Animal Care guidelines.

Cell Culture

HEK 293 cells were obtained from Thermo Fisher Scientific (Thermo Fisher Scientific, Ottawa, Ontario, Canada), and IPEC-J2 (ACC 701, RRID: CVCL_2246) were purchased from the DSMZ-German Collection of Microorganisms. Caco-2 cells were purchased from the American Type Culture Collection (ATCC, Manassas, Virginia, USA). For the generation of HEK 293 cells that stably express exogenous pCaSR (HEK-293-pCaSR cell line), plasmid pcDNA5/FRT-pCaSR was mixed up with pOG44 (Thermo Fisher Scientific) at a 9:1 ratio in Opti-MEM (Thermo Fisher Scientific) then were mixed with Opti-MEM containing Lipofectamine™ 2000 Transfection Reagent (Invitrogen, Fisher Scientific, Ottawa, Ontario, Canada) to get co-transfection complexes. After that, the co-transfection complexes were transfected into HEK 293 cells according to manufacturer instructions. At 48 h post-transfection, the complete medium was changed to a complete medium containing 200 ng/mL hygromycin B (Thermo Fisher Scientific). HEK 293 cells, HEK-293-pCaSR cells, IPEC-J2, and Caco-2 were all maintained in the 75 cm^2 flask at 37 °C in a humidified atmosphere of 5% CO_2 and 95% O_2. HEK 293 cells were maintained in high glucose Dulbecco's modified eagle medium (DMEM) (Invitrogen, Fisher Scientific) supplemented with 10% fetal bovine serum (FBS) (Hyclone, Canadian origin; Fisher Scientific, Ottawa, Ontario, Canada), penicillin (100 IU/mL), streptomycin (100 µg/mL) (Invitrogen, Fisher Scientific), while IPEC-J2 and Caco-2 were cultured in DMEM/Ham's F-12 (1:1) (Invitrogen, Fisher Scientific) with 10% FBS (Hyclone), penicillin (100 IU/mL), and streptomycin (100 µg/mL) (Invitrogen, Fisher Scientific). Culture medium was replaced every two to three days. When reaching 80 to 90% confluency, cells were collected for further analyses.

Animals and Sample Collection

Fresh ileum samples from three piglets were obtained from a study at the University of Manitoba (Choi et al., 2020). Weaned piglets (TN Tempo × TN70) with average body weight (BW ± SD) of 8.52 ± 0.11 kg at the age of 28 d were obtained from the Glenlea Swine Research Unit at the University of Manitoba and housed in individual pens in a temperature-controlled room within the T.K. Cheung Centre for Animal Science Research at the University of Manitoba. All piglets were allowed free access to feed and water. At the end of the experiment (day 12), piglets were anesthetized by an intramuscular injection of ketamine: xylazine (20:2 mg·kg^{-1} BW) and euthanized with a captive bolt gun. The abdomen was immediately opened to expose the whole gastrointestinal tract, and the ileum was pulled out quickly, excised, and divided into a piece of a 50-cm segment. The segment was quickly flushed three times with 70 mL of ice-cold "Phosphate-buffered-Phenylmethylsulfonyl fluoride (PMSF)- Dithiothreitol (DTT) saline" solution (0.2 mM PMSF, 0.5 mM DTT, 137 mM NaCl, 2.7 mM KCl, 10 mM Na_2HPO_4, and 1.8 mM KH_2PO_4, pH 7.4) for further cell isolation.

Porcine Intestinal Epithelial Cells Isolation

The Weiser distended intestinal sac technique was adopted in this study with a slight alteration to isolate the upper epithelial cells from the pig small intestine (Fan et al., 2001). The rinsed ileal segments were subsequently filled with about 200 mL of the oxygenated "Pre-isolation buffer" (0.2 mM PMSF, 0.5 mM DTT, 27 mM sodium citrate, 85 mM NaCl, 2.7 mM KCl, 5.6 mM Na_2HPO_4, and 8 mM KH_2PO_4; pH 7.4). The ends of the ileal segment were tied tightly and then placed in a 1L beaker containing the oxygenated "Phosphate-Buffered Saline" (PBS) (137 mM NaCl, 2.7 mM KCl, 10 mM Na_2HPO_4, and 1.8 mM KH_2PO_4, pH 7.4) for the incubation. The beaker was placed in a 37 °C incubator with a shaking water bath (50 cycles/min) for 30 min. After the incubation, the ileal segments were emptied and then filled with oxygenated "Cell isolation buffer" (1.5 mM Ethylenediaminetetraacetic acid (EDTA), 0.5 mM DTT, 137 mM NaCl, 2.7 mM KCl, 10 mM Na_2HPO_4, and 1.8 mM KH_2PO_4, pH 7.4) (Oates et al., 1997) for the isolation of villus epithelial cells. The beaker containing the ileal segments

were then put back to the same incubator and shook for 40 min. After that, the cell isolation buffer was collected and centrifuged at 400 × g for 2 min at 4 ℃and the fat and mucosa were gently removed.

Cell sorting of Enterocytes by Fluorescence-Activated Cell Sorting (FACS)

Isolated cells were resuspended with pre-cold DMEM, and cells were filtered by using a Sterile Nylon Net filter with 60 µm pore size (Millipore (Canada) Ltd., Etobicoke, Ontario, Ottawa, Canada). Subsequently, cells were washed once with pre-cold PBS and cells were centrifuged at 800 × g for 3 min at 4 ℃Cells pellet was then put into the PBS for cell counting. After being counted, cells were blocked in 5% goat serum (Jackson ImmunoResearch Laboratories, West Grove, Pennsylvania, USA) for 60 min at room temperature. After aspirating blocking solution, cells were incubated with an anti-sucrase-isomaltase antibody (sc-393424, Santa Cruz Biotechnology, Inc., Dallas, Texas, USA) at 1:100 dilution in PBS for 1 h at room temperature. The cross-reactivity of the anti-sucrase-isomaltase antibody was already validated in the porcine sample (Zhang et al., 2018) and in the IPEC-J2 cell in our pilot experiment (unpublished). After that, cells were rinsed three times in 1× PBS for 5 min each, followed by the incubation of cells with the second antibody Alexa Fluor® 488 AffiniPure Goat Anti-Mouse IgG (H+L) (115-545-166, Jackson ImmunoResearch Laboratories) diluted in PBS (1:500) for 30 min at room temperature in the dark. Cells were then rinsed three times with PBS for 5 min each, followed by the incubation with 4',6-diamidino-2-phenylindole (DAPI) (1:5000 diluted in PBS) (Thermo Fisher Scientific) for 5 min at room temperature. Cells were further rinsed three times in 1× PBS for 5 min each, before resuspending cells into cell sorting buffer (1×PBS +1% FBS + 2 mM EDTA). Cell sorting was then conducted by using a BD FACSCanto-II Digital Flow Cytometry Analyzer (BD Biosciences, San Jose, California, USA). After three times of cell sorting, isolated enterocytes were pooled together and stored in 100 µL lysis buffer provided by the RNA isolation kit (Invitrogen, Fisher Scientific) for further analysis.

RNA Extraction, cDNA Synthesis and Droplet Digital PCR (ddPCR)

RNA was isolated and purified by using RNA isolation kit RNAqueous Micro Total RNA Isolation Kit (Invitrogen), according to the manufacture's instruction. The concentration and OD260:OD280 ratio of extracted RNA samples were measured using a Nanodrop UV-Vis spectrophotometer 2000 (Thermo Scientific). All RNA samples were stored at -80°C for the cDNA synthesis. About 500 ng RNA was used for the cDNA synthesis by using an iScript cDNA Synthesis Kit (Biorad, Mississauga, Ontario, Canada) according to the manufacturer's instructions. The forward (F) and reverse primers for pCaSR were: CaSR-F (5'- GCCAAAGATCAGAACCTAG-3') and CaSR-R (5'-GCTGTTTATTTCCTCTATG-3'). As for ddPCR, 25 µL of PCR reaction mixture containing different levels of cDNA template (50-100 µg) were prepared. Each pCaSR primer (100 nmol/L) and 1× Evagreen Supermix (Biorad) and 20 µL of the above mixture were transferred into a sample well of the droplet generator cartridge (DG8 cartridges; Biorad). Droplet Generation Oil (70 µL) (Biorad) was added to the oil wells of DG8 cartridges. After that, droplets were obtained by employing the droplet generator (Biorad) and then they were gently transferred into a 96-well PCR plate (Biorad). The pCasR gene in the droplets was amplified by using a C1000 Touch thermal cycler (Biorad), according to the following thermal cycling protocol: 95°C for 5 min, 40 cycles of 95°C for 30 s and 58°C for 1 min, and followed by 4°C for 5 min, 90°C for 5 min and 4°C for 10 min. PCR end products were read by the QX200 droplet reader (Biorad), and data were analyzed by QuantaSoft (Biorad).

Library Preparation, and RNA Sequencing

RNA sequencing was performed by GENEWIZ Global Headquarters & NJ Lab (South Plainfield, New Jersey, USA) using Illumina HiSeq (Illumina, Inc., San Diego, California, USA) mRNA library preparation, at a 2 × 150 base-pair configuration (single index, per lane). Sequence reads were trimmed to remove possible adapter sequences and nucleotides with poor quality using Trimmomatic v.0.36 (Bolger et al., 2014). The trimmed reads were mapped to the Ensembl Sus scrofa 11.1 reference genome by using the STAR aligner v.2.5.2b (Dobin et al., 2013). Unique gene

hit counts were calculated by using featureCounts from the Subread package v.1.5.2 (Liao et al., 2013). Only unique reads that fell within exon regions were counted.

Immunofluorescence Staining and Western Blotting

The primary antibody against CaSR (ab137408) was used in immunofluorescence staining and western blotting. The immunogen sequence of this antibody and the sequence corresponding to the pCaSR have a very high similarity of 96%, implying the primary antibody against CaSR (ab137408) is predicted to be able to work with pCaSR. Moreover, the cross-reactivity of this antibody was also validated in our lab. Four types of cells (HEK 293 cells, Caco-2, IPEC-J2 and isolated intestinal epithelial cells) were fixed with 4% paraformaldehyde. The fixed cells were blocked in 5% goat serum for one hour at room temperature, and then cells were stained with an anti-CaSR antibody (ab137408, Abcam, Cambridge, Massachusetts, USA) (1:200) overnight; washed three times in PBS; stained for 1 hour with an Alexa Fluor 488 goat anti-rabbit antibody (A32731, 1:500, Thermal Scientific), and mounted with Vectashield mounting medium with DAPI (Vector Laboratories, Burlington, Ontario, Canada). Fluorescent images were recorded by using a Zeiss fluorescence microscope (Car-Zeiss Ltd., Toronto, Ontario, Canada).

For western blotting, HEK 293 cells, Caco-2, IPEC-J2 and isolated intestinal epithelial cells were rinsed with cold 1× PBS and scraped in pre-cold 1× RIPA lysis buffer (Sigma-Aldrich) which contains the 1× protease and phosphatase inhibitor cocktail (Thermo Scientific). After being centrifuged at 12,000 × g for 10 min at 4 °C, supernatants were collected for the total protein concentration assay. Total protein concentration was determined by utilizing a BCA protein assay kit (Thermo Scientific), and the standard curve was generated by using the bovine serum albumin (BSA) (fraction V). There were 70 µg proteins that were applied in the electrophoresis by using 4-15% Mini-PROTEAN® TGX Stain-Free™ Protein Gels (Bio-Rad), followed by the transfer with a nitrocellulose membrane (Bio-Rad). The blocking was conducted by using 5% skim milk powder in tris-buffered saline with 0.1% Tween 20 (TBST), and the membrane was incubated with rabbit anti-CaSR primary antibody

(ab137408, Abcam) that was diluted in 5% skim milk in TBST (1:2000) at 4 ºC overnight. The membrane was rinsed with TBST 3 times, and then the membrane was incubated with secondary antibody horseradish peroxidase-conjugated goat anti-rabbit IgG (324300, 1:4000, Thermo Scientific) which was diluted in 5% skim milk in TBST at room temperature for 1h. The membrane was visualized by using Clarity™ Western ECL Substrate (Bio-Rad), according to the manufacturer's instruction. The chemiluminescent signal densities were analyzed by utilizing the ChemiDoc MP imaging system (Bio-Rad).

RESULTS

Fluorescence-Activated Cell Sorting

Porcine enterocytes were characterized and sorted by immunofluorescence labeling and flow cytometry to obtain enterocytes from mixed isolated intestinal epithelial cells. In general, the mechanical method for isolating intestinal epithelial cells yielded large numbers of mixed heterogeneous cells, and the viability of isolated cells was good. According to flow cytometric analysis results (Figure 2), porcine enterocytes with a high level of surface sucrase-isomaltase expression profile were distinguished by sequential gating of cells, single cells, single live cells, and single porcine enterocytes. For isolated intestinal cells sample, 98.7% were identified as single cells, and 91.7% of single cells were gated as live cells. Among living cells, 94.9% of cells were negative for the enterocyte marker, while porcine enterocytes made up 3.3% of the live cells. About 320, 000 porcine intestinal enterocytes were harvested by FACS, and they were pooled together into a tube for the downstream RNA extraction and purification.

RNA Isolation and Purification from FACS Sorted Enterocytes

The RNA yield for isolated porcine intestinal enterocytes was about 11 ng/μL before the gDNA elimination using the RNA-isolation kit, and this value increased to 22 ng/μL after the gDNA elimination (Data not shown). Furthermore, the 260/280 ratio for isolated enterocytes RNA before the gDNA elimination was 2.1, but it became 1.98 after the gDNA elimination (Data not shown).

Identification of pCaSR in Isolated Porcine Enterocytes and IPEC-J2 by Droplet Digital PCR (ddPCR)

When conducting ddPCR, HEK 293 cells that did not express endogenous CaSR were used as the negative control, while HEK 293 cells that highly and stably express the exogenous pCaSR were employed as the positive control. In Figure 3, it is shown that there were no detectable copies of the pCaSR gene in both sorted enterocytes and IPEC-J2 at the different levels of cDNA tested, compared with the negative control group and positive control group.

Identification of pCaSR in Isolated Porcine Enterocytes and IPEC-J2 by RNA Sequencing

Based on the RNA sequencing results shown in Figure 4, the enterocytes-specific markers sucrase-isomaltase and maltase-glucoamylase were highly expressed in isolated enterocytes with the transcripts read counts of 7162 and 677, respectively, while these values were 27 and 696 in IPEC-J2 cells (Figure 4). As for CaSR, its transcripts in both sorted enterocytes and IPEC-J2 were undetectable since the transcripts read counts equaled to zero.

Identification of pCaSR in Isolated Porcine Enterocytes and IPEC-J2 by Immunofluorescence Staining and Western Blotting

The images in Figure 5A show intense fluorescence of the CaSR in the Caco-2, further supporting the expression of CaSR in Caco-2. Unlike the positive control group (Caco-2), the negative control group (HEK 293 cells) did not show the positive staining of CaSR, mirroring the fact that there is no endogenous expression of the CaSR in the HEK 293 cells. Furthermore, Figure 5A showed that there

was no intense positive staining of the CaSR in IPEC-J2 or intestinal epithelial cells, suggesting that the CaSR does not express in IPEC-J2 and porcine enterocytes.

The protein expression of CaSR in these four cell types was further investigated by Western blotting (Figure 5B), and the expected 280-kDa band representing the dimerized form of the CaSR in Caco-2 cells was confirmed. However, no bands were observed in either HEK 293 cells, IPEC-J2, or intestinal epithelial cells, indicating no CaSR protein expression detected in IPEC-J2 and porcine enterocytes.

DISCUSSION

As the most abundant cell type in the gut, enterocytes play pivotal roles in digesting and absorbing nutrients like calcium and amino acids from the intestinal lumen into the body (Farre et al., 2020). Plus, research on the physiological control of nutrient digestion and absorption has shown that G protein-coupled receptors (GPCRs) are closely involved in the sensing of a range of nutrients and other food components in the gastrointestinal tract (Reimann et al., 2012). As a class C member of GPCRs, CaSR also performs functions in nutrient sensing by activating different signalling pathways upon agonists stimulation (Liu et al., 2018b). Additionally, the calcium ion serves as the primary agonist for CaSR, and L-amino acids such as L-tryptophan have been identified as one of the positive modulators of CaSR (Geng et al., 2016). Besides, previous research also found the crosstalk between CaSR and dietary compounds such as vitamin D, since dietary vitamin D could upregulate CaSR expression (Aggarwal et al., 2016). Our previous study found a high pCaSR mRNA abundance in the porcine ileum (Zhao et al., 2019), conforming with the fact that the ileum is the main site of calcium absorption in pigs (Partridge, 1978). Although efforts have defined CaSR expression in different tissues among various species, limited data are available on CaSR expression in individual cell types (Feng et al., 2010). A previous study demonstrated that GPCRs are expressed in various types of cells

with different expression profiles (Insel et al., 2012). Thus, evaluating the average expression abundance in tissues might mask such heterogeneity (Insel et al., 2012). Moreover, research to unravel physiological activities in tissues need to be aided by data that identify the CaSR expression and features of individual cell types and what crosstalk happens among different cell types (Insel et al., 2012).

Approaches to identify the GPCRs expression in the individual cell type include real-time PCR, RNA sequencing, cDNA microarrays, immunohistochemistry, and immunofluorescence staining, among others (Insel et al., 2015; Sriram et al., 2019). Among those various methods, investigations that define receptor expression based on RNA expression are considered "unbiased," as those methods offer improved specificity compared with methods detecting protein expression levels (Insel et al., 2015). Although ddPCR is very sensitive and accurate, RNA sequencing was used to confirm the ddPCR results because RNA sequencing could detect multiple types of genes (such as the expression levels of CaSR and enterocyte-specific marker sucrase-isomaltase) in one sample simultaneously and also detect both known and novel transcripts of pCaSR. Hence, the expression of pCaSR in porcine ileal enterocytes, as well as IPEC-J2, has been verified through a combination of biological tools, which include FACS, ddPCR, and RNA sequencing used in this study. Notably, considering the higher expression level of pCaSR in the ileum, we isolated enterocytes from the pig ileum and detected the expression of pCaSR in ileal enterocytes.

Given those intestinal enterocytes are in the small and large intestine epithelium and represent more than 85% of the various epithelial cell types (Allaire et al., 2018), the upper epithelial cells in the ileum were isolated and collected in the current study. The porcine epithelial cell isolation method was modified from the protocol in early studies, which isolated intestinal epithelial cells along the crypt-villus axis (Oates et al., 1997; Yang et al., 2011). Based on the results of mixed isolated porcine intestinal epithelial cells, the portion of live cells was over 90%, suggesting that the viability of a mixed population of epithelial cells was high. This implies that the epithelial cells

isolation method employed in the present study is comparable with other methods, reproducible, and shares similar cell viability results (Chougule et al., 2012). Moreover, the epithelial cells isolation method employed in the current study has other advantages as it is easy to operate and time-efficient. Furthermore, it avoids the adverse effects of the enzyme treatment method like enzymatic digestion times that are difficult to control (Chougule et al., 2012).

Recent work has demonstrated that there are a set of brush border digestive enzymes embedded in the microvilli, and they control the final step in the digestion of dietary carbohydrates and proteins (Hooton et al., 2015). Those brush border digestive enzymes contain maltase-glucoamylase, sucrase-isomaltase, lactase, peptidases, and lipases (Van Beers et al., 1995). Among those digestive enzymes, sucrase-isomaltase has been used to mark absorptive enterocytes in the porcine small intestine and colon (Gonzalez et al., 2013). Hence, sucrase-isomaltase was employed in the current study to isolate enterocytes from the porcine ileum. Based on the flow cytometric analysis results, the percentage of porcine enterocytes was 3.3% of the live cells, lower than the data obtained in the human intestinal enterocytes isolation study (about 10-25%) (Chougule et al., 2012). The low isolation rate of enterocytes might be due to aborts (e.g., hardware aborts and software aborts) during the FACS (Chougule et al., 2012). Nevertheless, FACS is suitable for rare cell sorting (subpopulations of < 1%) when heterogeneous cell samples are being analyzed, reinforcing that FACS was appropriate for the small but detectable percentage of porcine live enterocytes obtained in this study.

The differences in the percentage of live porcine enterocytes and the percentages of human enterocytes could be explained by several aspects. Firstly, the different affinities to the primary antibody targeting the sucrase-isomaltase. The current study used the same primary antibody as in the human research mentioned above. However, the anti-sucrase-isomaltase antibody used in the current was originally designed to detect sucrase-isomaltase of the mouse, rat, and human origin. As indicated by the manufacturer's instruction, it could be that this antibody was of limited use for

detecting porcine sucrase-isomaltase marker. Currently, there is no porcine sucrase-isomaltase antibody. Once available, it is expected that the detection percentages of porcine live enterocytes would increase and be like the ones in human studies. Secondly, a higher criterion was used during the sorting to increase the purity of interested cells, which could lose many enterocytes and result in the low yield of isolated enterocytes. Lastly, to guarantee the cell viability of isolated enterocytes, the incubation time of the primary antibody was reduced from 2 h to 1 h at room temperature, which could also contribute to the low isolation rate of enterocytes. Nevertheless, the percentage of positive staining porcine enterocytes could still provide enough sorted enterocytes for CaSR gene quantification in the present study. Moreover, based on the RNA sequencing results, high expression levels of sucrase-isomaltase and maltase-glucoamylase were observed in isolated enterocytes, further identifying and confirming those epithelial cells obtained from FACS were porcine enterocytes. Hence, our results showed that sucrase-isomaltase was able to work as a good porcine enterocyte marker to isolate enterocytes from the mixed epithelial cells.

So far, the expression pattern of CaSR in enterocytes has been rarely explored, and the results from these studies are equivocal and inconsistent. According to early studies, CaSR was detected in human enterocytic cell lines such as Caco-2 and HT-29 and at the very base of the human colon crypt (Sheinin et al., 2000; Cheng et al., 2002; Liu et al., 2018a). Furthermore, a recent study also showed that the positive immunofluorescent staining of CaSR was found on the basolateral side of the villous cells and submucosal neurovascular structures in mice (Xu et al., 2020). Another study also documented the localization of CaSR on the basolateral membrane of the basal aspects of the villus epithelial cells in the rat small and large intestine by using immunohistochemistry (Chattopadhyay et al., 1998). Meanwhile, recent research also found that no consistent CaSR positive staining was found in most intestinal epithelial cells, except for the EECs, indicating the expression of CaSR in EECs rather than enterocytes (Modvig et al., 2021). Based on our results, except for Caco-2 cells, neither isolated porcine intestinal enterocytes nor the enterocyte-like cell line IPEC-J2 showed detectable

pCaSR. Hence, it is worth discussing what resulted in those contradictory reports on the expression of CaSR in the enterocytes.

Several potential reasons might explain the inconsistency between our study and those studies mentioned above. On the one hand, both Caco-2 and HT-29 belong to human colonic carcinoma cell lines, which are derived from patients with colon cancer, while both primary intestinal enterocytes and the enterocytic cell line IPEC-J2 were isolated from normal healthy piglets (Brosnahan and Brown, 2012). Furthermore, both Caco-2 and HT-29 are transformed-cell lines, but IPEC-J2 is non-transformed, which makes Caco-2 and HT-29 show different characteristics from the typical intestinal enterocytes. Also, although when grown in culture, Caco-2 and HT-29 could differentiate into enterocytes, these enterocytes are of human colonic origin as opposed to IPEC-J2 and enterocytes isolated in our study that were of small intestine origin and therefore functional differences may be present between these two types of enterocytes. For example, receptors for peptide YY (PYY) or neuropeptide Y, which have been confirmed in normal intestinal epithelial cells, have no detectable expression level in HT-29 (Kleiveland, 2015). Moreover, even though many digestive enzymes and transporters present in Caco-2 have also been identified in normal human intestinal epithelial cells, it has been reported that differences in gene expression patterns for transporters, nuclear receptors, and transcription factors exist between Caco-2 and normal human intestinal epithelial cells (Bourgine et al., 2012). Furthermore, the CaSR expression was also different in the normal colonic crypts than in the abnormal crypts, as a more substantial degree of CaSR staining was observed in normal colonic epithelial cells (Chakrabarty et al., 2003). Like Caco-2, HT-29 in its differentiated phenotype cannot be compared with absorptive enterocytes because of various gene expression profile differences, such as hydrolases and ion transport properties (Hekmati et al., 1990). All these aspects might contribute to the different expression profiles of receptors such as CaSR in the human colonic enterocyte-like cell lines and porcine ileal enterocytes.

It is also possible that the contradictory results may be due to the limitations of techniques adopted in different studies. Technically, primary intestinal enterocytes are particularly difficult to study because of the rapid onset of cell death after detachment from the intestine (Frisch and Screaton, 2001). In this context, when detecting the CaSR expression in the intestine, most researchers tend to conduct the detection work without isolating enterocytes from the intestine. That might exacerbate the biased results if antibody-based approaches with questionable specificity were employed. Specifically, one study identified the transcripts and protein of CaSR in both apical and basolateral sides of epithelial cells isolated from rat colonic epithelium by using immunohistochemistry and immunofluorescence, and other studies confirmed the expression of CaSR at the very base of the human colon crypt (Cheng et al., 2002; Chakrabarty et al., 2003). Positive immunofluorescent staining of CaSR on the basolateral side of the villous cells combined with the high abundance of enterocytes in intestinal epithelial cells made some researchers suspect that CaSR would be expressed in the basolateral side of the enterocytes (Cheng et al., 2002). Notably, those researchers' speculation was based on data obtained by utilizing immunofluorescent staining without using a specific marker that could characterize the enterocytes. Intestinal epithelial cells consist of different types of cells, including Paneth cells, goblet cells as well as EECs (Iamartino et al., 2018). In fact, the mRNA of CaSR was identified in the EECs such as gastrin-secreting G cells and the cholecystokinin-secreting K cells, as well as Paneth cells (Reimann et al., 2012). Therefore, the positive staining of CaSR in the epithelium of the small intestine might be caused by the positive staining of CaSR in these other cell types rather than intestinal enterocytes. Moreover, all those findings mentioned above were generated based on the antibody-based techniques without the relevant mRNA detection to verify their results further. For example, it has been reported the protein expression of CaSR in IPEC-J2 cells by using the western blotting analysis (Liu et al., 2018b, Gao et al., 2021), without the confirmation of mRNA. Here, our current study addressed both issues (primary enterocytes isolation and "unbiased" detection methods) by employing FACS, ddPCR, and RNA sequencing.

Furthermore, there is also other evidence that might support our findings in this present study. It is well documented that CaSR contains three main domains: an extracellular domain, seven transmembrane domains, and one intracellular domain (Hendy and Canaff, 2016). Studies reported that the extracellular domain is the primary binding site for CaSR ligands, and CaSR ligands include extracellular calcium ions, free L-amino acids, spermine (Zhao et al., 2020). If the CaSR is located at the basolateral membrane of enterocytes in the small intestine, it only could sense its ligands that have been released in the basal membrane by intestinal epithelial cells and then induce the down-stream signaling pathways. This speculation has been mentioned only by a few researchers based on the results obtained by Chattopadhyay et al. (1998) and studies conducted on oxyntopeptic cells (Caroppo et al., 2001; Gerbino and Colella, 2018). However, it is acknowledged that there is a lack of sufficient data to support this speculation (Wongdee et al., 2019). Lastly, even though the amino acid sequences of pCaSR share a high identity with human CaSR, there are variances between them, which might also make the expression pattern of CaSR located in intestinal enterocytes different in humans and pigs (Zhao et al., 2019).

Considering that there was no detectable expression of pCaSR in the ileal enterocytes in the current study, we speculated that the pCaSR might participate in regulating the absorption of calcium and other nutrients via paracrine regulation. Furthermore, the activation of CaSR in EECs has been demonstrated to stimulate the release of gut hormones (such as CCK, GLP-1, and GLP-2), and those gut peptides can modulate tight junctions in the intestine (Burrin et al., 2000), which subsequently might affect the paracellular absorption of dietary calcium, as well as the transportation of other nutrients. Hence, the roles of identified pCaSR ligands on nutrient absorption and gut barrier function could be explored by using the EECs-enterocytes co-culture system to mimic paracrine functions in further studies. Additionally, as the expression of pCaSR was only invested in the ileum in weaned piglets in the current study, previous research observed the segregated expression of receptors in the intestinal tract (Price et al., 2018). Specifically, the early study revealed that the expression of the Toll-like receptor varied remarkably in the intestine with distinct

spatial and temporal patterns (Price et al., 2018). In this context, the expression pattern of pCaSR in the absorptive enterocytes in other intestinal segments except for the ileum and those in other stages of swine production could be further explored in future studies.

In summary, porcine ileal enterocytes could be obtained by using FACS with sucrase-isomaltase as an enterocyte marker. Furthermore, the pCaSR is not expressed in either isolated ileal enterocytes or IPEC-J2. Our study provides new insights, which lay a foundation for future work exploring the role of pCaSR in regulating nutrient absorption in the small intestine.

DISCLOSURES

No conflicts of interest, financial or otherwise, are declared by the authors.

LITERATURE CITED

Aggarwal, A., J. Höbaus, S, Tennakoon, M. Prinz-Wohlgenannt, J. Graça, S. A. Price, and E. Kállay. 2016. Active vitamin D potentiates the anti-neoplastic effects of calcium in the colon: a cross talk through the calcium-sensing receptor. J. Steroid Biochem. Mol. Biol. 155, 231–238. doi: 10.1016/j.jsbmb.2015.02.006.

Allaire, J. M., S. M. Crowley, H. T. Law, S. Y. Chang, H. J. Ko, and B. A. Vallance. 2018. The intestinal epithelium: central coordinator of mucosal immunity. Trends. Immunol. 39(9):677-696. doi: 10.1016/j.it.2018.04.002.

Bolger, A. M., M. Lohse, and B. Usadel. 2014. Trimmomatic: a flexible trimmer for Illumina sequence data. Bioinformatics. 30(15):2114-2120. doi: 10.1093/bioinformatics/btu170.

Bourgine, J., I. Billaut-Laden, M. Happillon, J. M. Lo-Guidice, V. Maunoury, M. Imbenotte, and F. Broly. 2012. Gene expression profiling of systems involved in the metabolism and the disposition of xenobiotics: comparison between human intestinal biopsy samples and colon cell lines. Drug. Metab. Dispos. 40(4):694-705. doi: 10.1124/dmd.111.042465.

Brosnahan, A. J., and D. R. Brown. 2012. Porcine IPEC-J2 intestinal epithelial cells in microbiological investigations. Vet. Microbiol. 156(3-4):229-237. doi: 10.1016/j.vetmic.2011.10.017.

Bullen, T. F., S. Forrest, F. Campbell, A. R. Dodson, M. J. Hershman, D. M. Pritchard, J. R.

Turner, M. H. Montrose, and A. J. Watson. 2006. Characterization of epithelial cell shedding from human small intestine. Lab. Invest. 86(10):1052-1063. doi: 10.1038/labinvest.3700464.

Burrin, D. G., B. Stoll, R. Jiang, Y. Petersen, J. Elnif, R. K. Buddington, M. Schmidt, J. J. Holst, B. Hartmann, and P. T. Sangild. 2000. GLP-2 stimulates intestinal growth in premature TPN-fed pigs by suppressing proteolysis and apoptosis. Am. J. Physiol. Gastrointest. Liver. Physiol. 279(6):G1249-1256. doi: 10.1152/ajpgi.2000.279.6.G1249

Busslinger, G. A., B. L. A. Weusten, A. Bogte, H. Begthel, L. A. A. Brosens, and H. Clevers. 2021. Human gastrointestinal epithelia of the esophagus, stomach, and duodenum resolved at single-cell resolution. Cell. Rep. 34(10):108819. doi: 10.1016/j.celrep.2021.108819.

Canadian Council on Animal Care (CCAC) Guidelines 2009. CCAC guidelines on: the care and use of farm animals in research, teaching and testing. Ottawa, ON, Canada: CCAC.

Caroppo, R., A. Gerbino, L. Debellis, O. Kifor, D. I. Soybel, E. M. Brown, A. M. Hofer, and S. Curci. 2001. Asymmetrical, agonist-induced fluctuations in local extracellular Ca^{2+} in intact polarized epithelia. EMBO. J. 20(22):6316-6326. doi: 10.1093/emboj/20.22.6316.

Chakrabarty, S., V. Radjendirane, H. Appelman, and J. Varani. 2003. Extracellular calcium and calcium sensing receptor function in human colon carcinomas: promotion of E-cadherin expression and suppression of beta-catenin/TCF activation. Cancer. Res. 63(1):67-71.

Chattopadhyay, N., I. Cheng, K. Rogers, D. Riccardi, A. Hall, R. Diaz, S. C. Hebert, D. I. Soybel, and E. M. Brown. 1998. Identification and localization of extracellular Ca^{2+}-

sensing receptor in rat intestine. Am. J. Physiol. 274(1):G122-130. doi: 10.1152/ajpgi.1998.274.1.G122.

Cheng, S. X., M. Okuda, A. E. Hall, J. P. Geibel, and S. C. Hebert. 2002. Expression of calcium-sensing receptor in rat colonic epithelium: evidence for modulation of fluid secretion. Am. J. Physiol. Gastrointest. Liver. Physiol. 283(1):G240-250. doi: 10.1152/ajpgi.00500.2001.

Choi, J., L. Wang, S. Liu, P. Lu, X. Zhao, H. Liu, L. Lahaye, E. Santin, S. Liu, M. Nyachoti, and C. Yang. 2020. Effects of a microencapsulated formula of organic acids and essential oils on nutrient absorption, immunity, gut barrier function, and abundance of enterotoxigenic *Escherichia coli* F4 in weaned piglets challenged with *E. coli* F4. J. Anim. Sci. 98(9). doi: 10.1093/jas/skaa259.

Chougule, P., G. Herlenius, N. M. Hernandez, P. B. Patil, B. Xu, and S. Sumitran-Holgersson. 2012. Isolation and characterization of human primary enterocytes from small intestine using a novel method. Scand. J. Gastroenterol. 47(11):1334-1343. doi: 10.3109/00365521.2012.708940.

Dobin, A., C. A. Davis, F. Schlesinger, J. Drenkow, C. Zaleski, S. Jha, P. Batut, M. Chaisson, and T. R. Gingeras. 2013. STAR: ultrafast universal RNA-seq aligner. Bioinformatics. 29(1):15-21. doi: 10.1093/bioinformatics/bts635.

Engelstoft, M. S., W. M. Park, I. Sakata, L. V. Kristensen, A. S. Husted, S. Osborne-Lawrence, P. K. Piper, A. K. Walker, M. H. Pedersen, M. K. Nohr, J. Pan, C. J. Sinz, P. E. Carrington, T. E. Akiyama, R. M. Jones, C. Tang, K. Ahmed, S. Offermanns, K. L. Egerod, J. M. Zigman, and T. W. Schwartz. 2013. Seven transmembrane G protein-coupled receptor repertoire of gastric ghrelin cells. Mol. Metab. 2(4):376-392. doi: 10.1016/j.molmet.2013.08.006.

Fan, M. Z., B. Stoll, R. Jiang, and D. G. Burrin. 2001. Enterocyte digestive enzyme activity

along the crypt-villus and longitudinal axes in the neonatal pig small intestine. J. Anim. Sci. 79(2):371-381. doi: 10.2527/2001.792371x.

Farre, R., M. Fiorani, S. Abdu Rahiman, and G. Matteoli. 2020. Intestinal permeability, inflammation and the role of nutrients. Nutrients. 12(4). doi: 10.3390/nu12041185.

Feng, J., C. D. Petersen, D. H. Coy, J. K. Jiang, C. J. Thomas, M. R. Pollak, and S. A. Wank. 2010. Calcium-sensing receptor is a physiologic multimodal chemosensor regulating gastric G-cell growth and gastrin secretion. Proc. Natl. Acad. Sci. U S A. 107(41):17791-17796. doi: 10.1073/pnas.1009078107.

Frisch, S., and Screation,R.A. 2001. Anoikis mechanisms. Curr. Opin. Cell. Biol. 13:555-562. doi: 10.1016/S0955-0674(00)00251-9.

Gao, N., X. Dou, T. Yin, Y. Yang, D. Yan, Z. Ma, C. Bi, and A. Shan. 2021. Tryptophan promotes intestinal immune defense through calcium-sensing receptor (CaSR)-dependent metabolic pathways. J. Agric. Food. Chem. 69(45):13460-13473. doi: 10.1021/acs.jafc.1c05820.

Geng, Y., L. Mosyak, I. Kurinov, H. Zuo, E. Sturchler, T. C. Cheng, P. Subramanyam, A. P. Brown, S. C. Brennan, H. C. Mun, M. Bush, Y. Chen, T. X. Nguyen, B. Cao, D. D. Chang, M. Quick, A. D. Conigrave, H. M. Colecraft, P. McDonald, and Q. R. Fan. 2016. Structural mechanism of ligand activation in human calcium-sensing receptor. Elife. 5. doi: 10.7554/eLife.13662.

Gerbino, A., and M. Colella. 2018. The different facets of extracellular calcium sensors: old and new concepts in calcium-sensing receptor signalling and pharmacology. Int. J. Mol. Sci. 19(4). doi: 10.3390/ijms19040999.

Gonzalez, L. M., I. Williamson, J. A. Piedrahita, A. T. Blikslager, and S. T. Magness. 2013. Cell lineage identification and stem cell culture in a porcine model for the study of intestinal epithelial regeneration. PLoS One. 8(6):e66465. doi:

10.1371/journal.pone.0066465.

Hekmati, M., Y. Ben-Shaul, and S. Polak-Charcon. 1990. A morphological study of a human adenocarcinoma cell line (HT29) differentiating in culture. Similarities to intestinal embryonic development. Cell Differentiation and Development. 31(3):207-218. doi: 10.1016/0922-3371(90)90133-h.

Hendy, G. N., and L. Canaff. 2016. Calcium-sensing receptor gene: regulation of expression. Front. Physiol. 7:394. doi: 10.3389/fphys.2016.00394.

Hooton, D., R. Lentle, J. Monro, M. Wickham, and R. Simpson. 2015. The secretion and action of brush border enzymes in the mammalian small intestine. Rev. Physiol. Biochem. Pharmacol. 168:59-118. doi: 10.1007/112_2015_24.

Iamartino, L., T. Elajnaf, E. Kallay, and M. Schepelmann. 2018. Calcium-sensing receptor in colorectal inflammation and cancer: current insights and future perspectives. World. J. Gastroenterol. 24(36):4119-4131. doi: 10.3748/wjg.v24.i36.4119.

Insel, P. A., A. Snead, F. Murray, L. Zhang, H. Yokouchi, T. Katakia, O. Kwon, D. Dimucci, and A. Wilderman. 2012. GPCR expression in tissues and cells: are the optimal receptors being used as drug targets? Br. J. Pharmacol. 165(6):1613-1616. doi: 10.1111/j.1476-5381.2011.01434.x.

Insel, P. A., A. Wilderman, A. C. Zambon, A. N. Snead, F. Murray, N. Aroonsakool, D. S. McDonald, S. Zhou, T. McCann, L. Zhang, K. Sriram, A. M. Chinn, A. V. Michkov, R. M. Lynch, A. C. Overland, and R. Corriden. 2015. G protein-coupled receptor (GPCR) expression in native cells: "Novel" endoGPCRs as physiologic regulators and therapeutic targets. Mol. Pharmacol. 88:181-187. doi: 10.1124/mol.115.098129.

Kleiveland, C. R. 2015. Co-cultivation of Caco-2 and HT-29MTX. In: K. Verhoeckx, P. Cotter, I. Lopez-Exposito, C. Kleiveland, T. Lea, A. Mackie, T. Requena, D. Swiatecka and H. Wichers, editors, The impact of food bioactives on health: *in vitro*

and *ex vivo* models, Cham (CH). p. 135-140. doi: 10.1007/978-3-319-16104-4.

Liao, Y., G. K. Smyth, and W. Shi. 2013. The Subread aligner: fast, accurate and scalable read mapping by seed-and-vote. Nucleic. Acids. Res. 41(10):e108. doi: 10.1093/nar/gkt214.

Liu, G., W. Cao, G. Jia, H. Zhao, X. Chen, and J. Wang. 2018a. Calcium-sensing receptor in nutrient sensing: an insight into the modulation of intestinal homoeostasis. Br. J. Nutr. 120(8):881-890. doi: 10.1017/S0007114518002088.

Liu, H., Tan, B., Huang, B., Li, J., Wang, J., Liao, P., Guan, G., Ji, P., and Y. Yin. 2018b. Involvement of calcium-sensing receptor activation in the alleviation of intestinal inflammation in a piglet model by dietary aromatic amino acid supplementation. Br. J. Nutr. 120(12), 1321–1331. doi:10.1017/S0007114518002891.

Mace, O. J., J. Affleck, N. Patel, and G. L. Kellett. 2007. Sweet taste receptors in rat small intestine stimulate glucose absorption through apical GLUT2. J. Physiol. 582(Pt 1):379-392. doi: 10.1113/jphysiol.2007.130906.

Mehra, A., K. H. Lee, and V. Hatzimanikatis. 2003. Insights into the relation between mRNA and protein expression patterns: I. theoretical considerations. Biotechnol. Bioeng. 84(7):822-833. doi: 10.1002/bit.10860.

Mine, Y., and H. Zhang. 2015. Calcium-sensing receptor (CaSR)-mediated anti-inflammatory effects of L-amino acids in intestinal epithelial cells. J. Agric. Food. Chem. 63(45):9987-9995. doi: 10.1021/acs.jafc.5b03749.

Modvig, I. M., R. E. Kuhre, S. L. Jepsen, S. F. S. Xu, M. S. Engelstoft, K. L. Egerod, T. W. Schwartz, C. Orskov, M. M. Rosenkilde, and J. J. Holst. 2021. Amino acids differ in their capacity to stimulate GLP-1 release from the perfused rat small intestine and stimulate secretion by different sensing mechanisms. Am. J. Physiol. Endocrinol. Metab. 320(5):E874-E885. doi: 10.1152/ajpendo.00026.2021.

Oates, P. S., C. Thomas, and E. H. Morgan. 1997. Characterization of isolated duodenal epithelial cells along a crypt-villus axis in rats fed diets with different iron content. J. Gastroenterol. Hepatol. 12(12):829-838. doi: 10.1111/j.1440-1746.1997.tb00380.x.

Ohsu, T., Y. Amino, H. Nagasaki, T. Yamanaka, S. Takeshita, T. Hatanaka, Y. Maruyama, N. Miyamura, and Y. Eto. 2010. Involvement of the calcium-sensing receptor in human taste perception. J. Biol. Chem. 285(2):1016-1022. doi: 10.1074/jbc.M109.029165.

Partridge, I. G. 1978. Studies on digestion and absorption in the intestines of growing pigs. 3. Net movements of mineral nutrients in the digestive tract. Br. J. Nutr. 39(3):527-537. doi: 10.1079/bjn19780068.

Price, A. E., Shamardani, K., Lugo, K. A., Deguine, J., Roberts, A. W., Lee, B. L., and Barton, G. M. 2018. A map of toll-like receptor expression in the intestinal epithelium reveals distinct spatial, cell type-specific, and temporal patterns. Immunity. 49(3):560–575. doi: 10.1016/j.immuni.2018.07.016.

Reimann, F., G. Tolhurst, and F. M. Gribble. 2012. G-protein-coupled receptors in intestinal chemosensation. Cell. Metab. 15(4):421-431. doi: 10.1016/j.cmet.2011.12.019.

Sheinin, Y., E. Kallay, F. Wrba, S. Kriwanek, M. Peterlik, and H. S. Cross. 2000. Immunocytochemical localization of the extracellular calcium-sensing receptor in normal and malignant human large intestinal mucosa. J. Histochem. Cytochem. 48(5):595-602. doi: 10.1177/002215540004800503.

Sriram, K., S. Z. Wiley, K. Moyung, M. W. Gorr, C. Salmeron, J. Marucut, R. P. French, A. M. Lowy, and P. A. Insel. 2019. Detection and quantification of GPCR mRNA: an assessment and implications of data from high-content methods. ACS Omega. 4(16):17048-17059. doi: 10.1021/acsomega.9b02811.

Umar, S. 2010. Intestinal stem cells. Curr. Gastroenterol. Rep. 12(5):340-348. doi: 10.1007/s11894-010-0130-3.

Van Beers, E. H., H. A. Buller, R. J. Grand, A. W. Einerhand, and J. Dekker. 1995. Intestinal brush border glycohydrolases: structure, function, and development. Crit. Rev. Biochem. Mol. Biol. 30(3):197-262. doi: 10.3109/10409239509085143.

Wongdee, K., M. Rodrat, J. Teerapornpuntakit, N. Krishnamra, and N. Charoenphandhu. 2019. Factors inhibiting intestinal calcium absorption: hormones and luminal factors that prevent excessive calcium uptake. J. Physiol. Sci. 69(5):683-696. doi: 10.1007/s12576-019-00688-3.

Xu, J., A. Zeug, B. Riederer, S. Yeruva, O. Griesbeck, H. Daniel, B. Tuo, E. Ponimaskin, H. Dong, and U. Seidler. 2020. Calcium-sensing receptor regulates intestinal dipeptide absorption via Ca^{2+} signaling and IKCa activation. Physiol. Rep. 8(1):e14337. doi: 10.14814/phy2.14337.

Yang, C., D. M. Albin, Z. Wang, B. Stoll, D. Lackeyram, K. C. Swanson, Y. Yin, K. A. Tappenden, Y. Mine, R. Y. Yada, D. G. Burrin, and M. Z. Fan. 2011. Apical Na^{+}-D-glucose cotransporter 1 (SGLT1) activity and protein abundance are expressed along the jejunal crypt-villus axis in the neonatal pig. Am. J. Physiol. Gastrointest. Liver. Physiol. 300(1):G60-70. doi: 10.1152/ajpgi.00208.2010.

Zhang, H., J. Kovacs-Nolan, T. Kodera, Y. Eto, and Y. Mine. 2015. gamma-Glutamyl cysteine and gamma-glutamyl valine inhibit TNF-alpha signaling in intestinal epithelial cells and reduce inflammation in a mouse model of colitis via allosteric activation of the calcium-sensing receptor. Biochim. Biophys. Acta. 1852(5):792-804. doi: 10.1016/j.bbadis.2014.12.023.

Zhang, Q., Ke, H., Blikslager, A., Fujita, T., & Yoo, D. 2018. Type III interferon restriction by porcine epidemic diarrhea virus and the role of viral protein nsp1 in IRF1 signaling. J. virol. 92(4), e01677-17.

Zhao, W., Z. Zhang, L. Zheng, C. You, H. Chi, T. Zhang, and G. Xu. 2020. Calcium-sensing

receptor activating ERK1/2 and PI3K-Akt pathways to induce the proliferation of osteosarcoma cells. Clin Exp. Pharmacol. Physiol. 47(3):517-519. doi: 10.1111/1440-1681.13209.

Zhao, X., B. Schindell, W. Li, L. Ni, S. Liu, C. U. B. Wijerathne, J. Gong, C. M. Nyachoti, K. O, and C. Yang. 2019. Distribution and localization of porcine calcium sensing receptor in different tissues of weaned piglets. J. Anim. Sci. 97(6):2402-2413. doi: 10.1093/jas/skz096.

FIGURE LEGENDS

Figure 1. Proposal model of nutrient sensing via the calcium-sensing receptor (CaSR) in enterocytes and enteroendocrine cells (EECs) (Created with BioRender.com). AM, apical membrane; BLM, basolateral membrane; cAMP, cyclic adenosine monophosphate; CCK, cholecystokinin; GLP-1, glucagon-like peptide 1; GLP-2, glucagon-like peptide 2; PKA, protein kinase A; PKC, protein kinase C; PYY, peptide YY.

Figure 2. Flow cytometry isolation of primary porcine enterocytes: Fluorescence-activated cell sorting (FACS) images demonstrate the gating strategy used to isolate porcine enterocytes. Events likely to represent single cells were selected on their size and relative dimensions, followed by dead cell exclusion using DAPI. As mentioned in materials and methods, Alexa fluor 488 dye conjugated to the primary antibody Sucrase-Isomaltase Antibody (A-12), which was used to mark porcine enterocytes; thus, Alexa fluor 488^{+} represents porcine enterocytes.

Figure 3. A representative image (events from QuantaLife software) of calcium-sensing receptor (CaSR) expression detection in sorted enterocytes and IPEC-J2 by using droplet digital PCR: A01 presents negative control with 50 ng cDNA input (HEK 293 cell which does not express endogenous CaSR was used to be negative control); A02 represents isolated porcine intestinal enterocytes with 200 ng cDNA input; A03 represents isolated porcine intestinal enterocytes with 100 ng cDNA input; A04 represents isolated porcine intestinal enterocytes with 50 ng cDNA input; A05 represents IPEC-J2 cells with 100 ng cDNA input; A06 represents IPEC-J2 cells with 50 ng cDNA input; A07 represents positive control (HEK 293 cell line which stably expresses the exogenous pCaSR) with 50 ng cDNA input. The channel amplitudes are plotted on Y-axis, whereas the events (number of droplets) are plotted on X-axis.

Figure 4. Detection of calcium-sensing receptor (CaSR) and enterocytes-specific markers in IPEC-J2 and isolated enterocytes by using RNA sequencing. SI: sucrase-isomaltase; MAG: maltase-glucoamylase.

Figure 5. Detection of calcium-sensing receptor (CaSR) in HEK 293, Caco-2, IPEC-J2, and isolated epithelial cells by using immunofluorescence staining and western blotting; (A) CaSR was detected with a primary antibody Anti-CaSR antibody and an AlexaFluor®488-conjugated secondary antibody; nuclei were stained with 4',6-diamidino-2-phenylindole (DAPI) (blue). The right panel is the merged image of the left and middle panels and scale bar is 20 µm; (B) protein lysates (70 µg) from HEK 293 cells (first lane), Caco-2 cells (second lane), IPEC-J2 (third lane), and isolated epithelial cells (fourth lane).

Figure 1

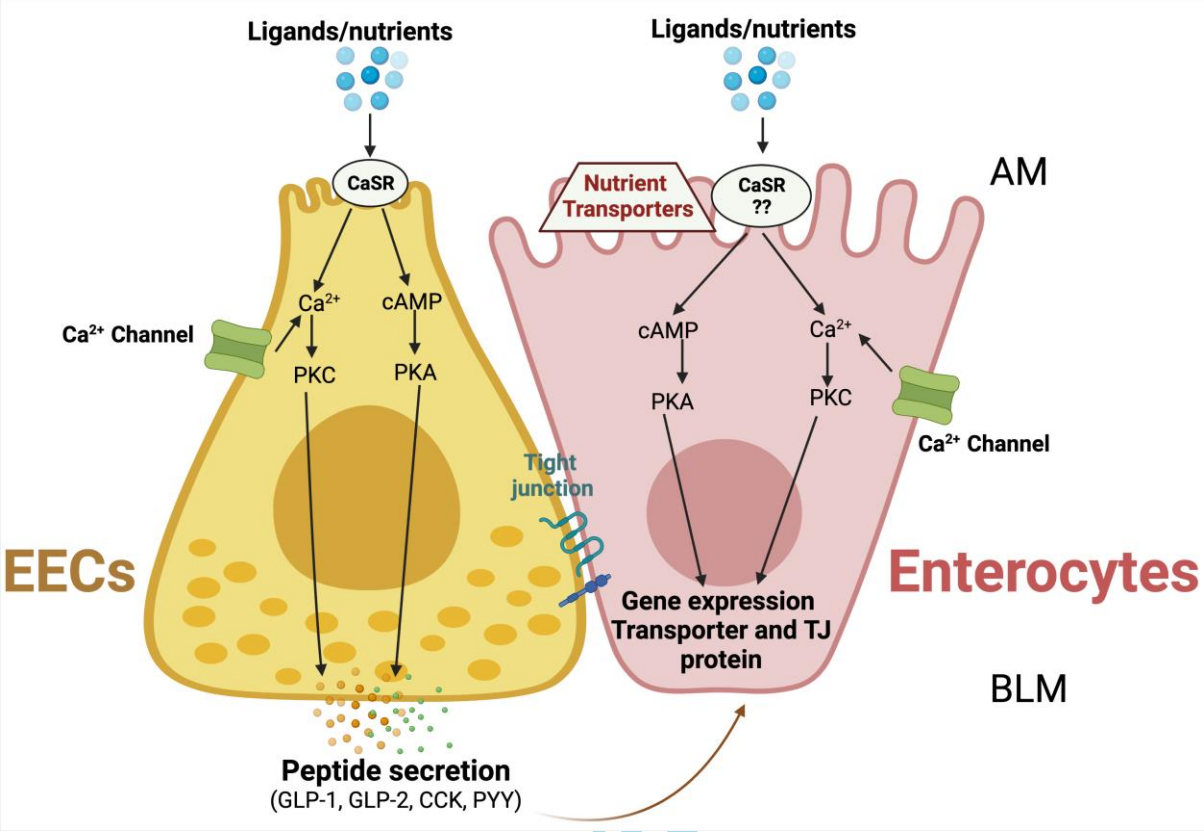

Figure 2

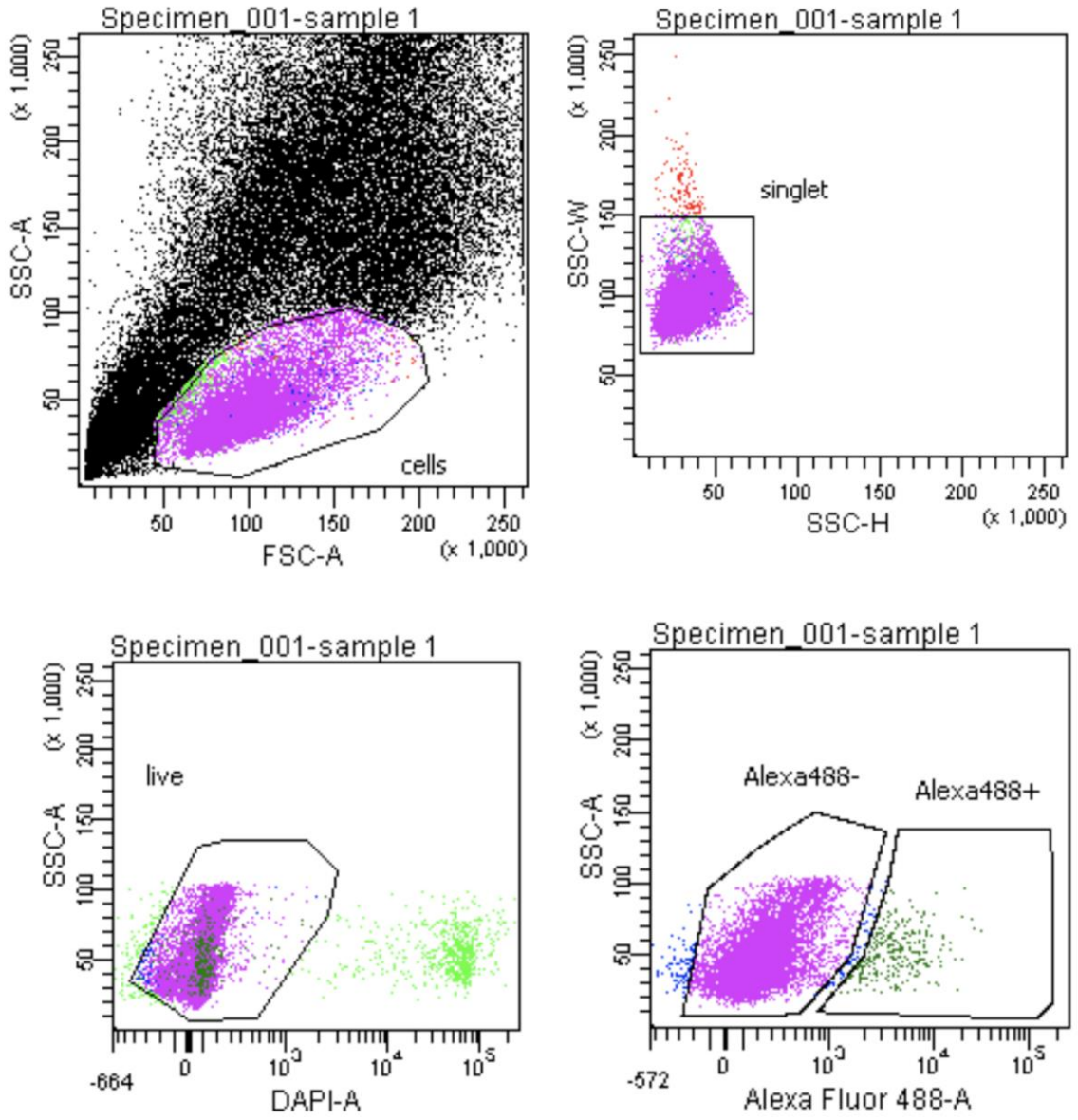

Figure 3

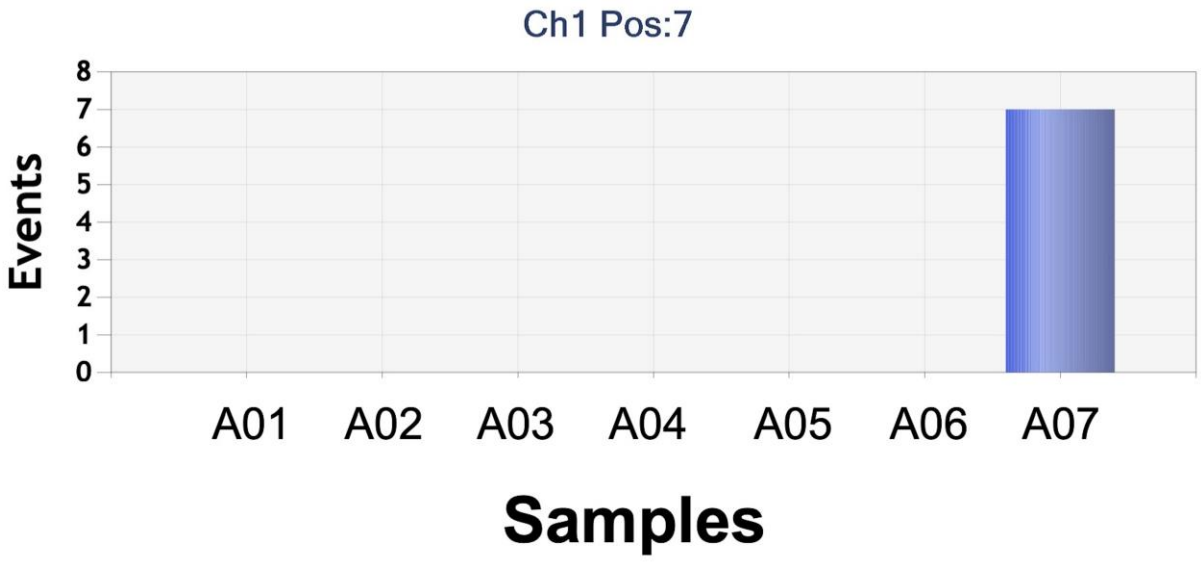

Figure 4

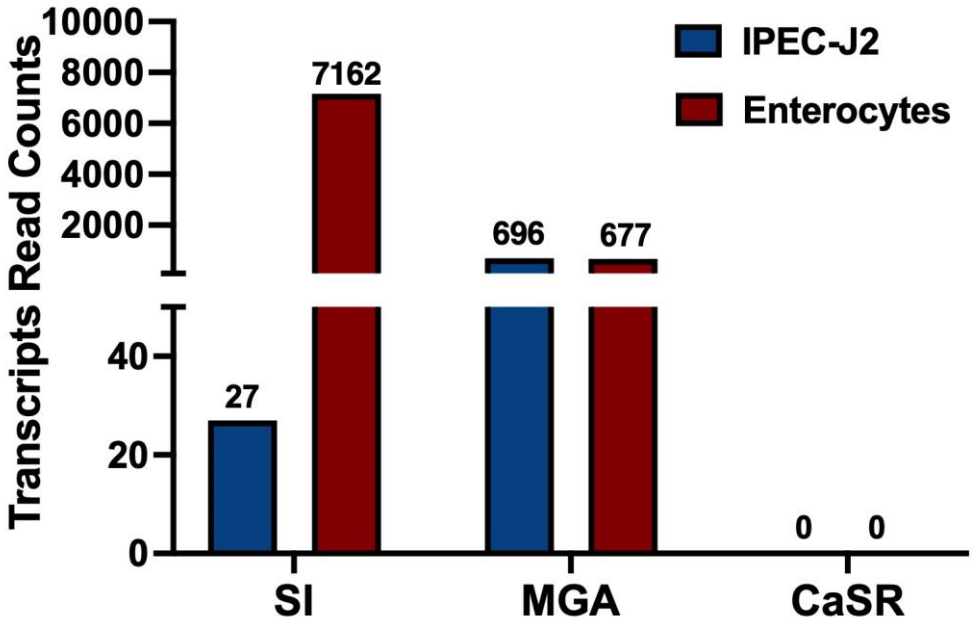

Figure 5